Sains Malaysiana 52(11)(2023): 3189-3209
http://doi.org/10.17576/jsm-2023-5211-13

Adsorption of Diclofenac from Aqueous Solution by Amine-Functionalized Poly(Acrylonitrile-*Co*-Acrylic Acid) Microparticles Adsorbent

(Penjerapan Diklofenak daripada Larutan Berair oleh Penjerap Mikrozarah Berfungsi Amine (Acrylonitrile-*ko*-Acrylic Acid))

Zakira Amalin Mohamad[1], Siti Nurul Ain Md Jamil[1,2,*], Nur Nida Syamimi Subri[1], Farhana Syakirah Ismail[1] & Rusli Daik[3,4]

[1]*Department of Chemistry, Faculty of Science, Universiti Putra Malaysia, 43400 UPM Serdang, Selangor, Malaysia*
[2]*Centre for Foundation Studies in Science of Universiti Putra Malaysia, 43400 UPM Serdang, Selangor, Malaysia*
[3]*Department of Chemical Sciences, Faculty of Science and Technology, Universiti Kebangsaan Malaysia, 43600 UKM Bangi, Selangor, Malaysia*
[4]*Institute of Microengineering and Nanoelectronics, Universiti Kebangsaan Malaysia, 43600 UKM Bangi, Selangor, Malaysia*

Received: 28 July 2023/Accepted: 25 October 2023

ABSTRACT

In this study, the synthesis of poly(acrylonitrile) (PAN) and poly(acrylonitrile-*co*-acrylic acid) (poly(ACN-*co*-AAc)) was carried out *via* redox polymerization, using sodium bisulphate (SBS) and potassium persulphate (KPS) as initiators. Subsequently, the resulting poly(ACN-*co*-AAc) was functionalized with ethanolamine (ETA) and ethylenediamine (EDA) to utilize as adsorbents for the removal of diclofenac from an aqueous solution. Both unfunctionalized and functionalized poly(ACN-*co*-AAc) were characterized using Fourier-Transform Infrared (FTIR) spectroscopy, Scanning Electron Microscope (SEM), Thermogravimetric Analysis (TGA), and Brunauer-Emmett-Teller (BET) analysis. The effects of pH, initial concentration of diclofenac solution, contact time, and adsorbent dosage were investigated during the adsorption process. The isotherm data were best fitted by the Langmuir model, indicating a mono-layered adsorption mechanism. The maximum adsorption capacities obtained from the Langmuir equation were higher for ETA-functionalized poly(ACN-*co*-AAc) at 120.5 mg/g, as compared to EDA-functionalized poly(ACN-*co*-AAc) at 80.6 mg/g. The experimental kinetic results showed that the pseudo-second-order model was a good fit for describing the adsorption rate of diclofenac for both ETA-functionalized poly(ACN-*co*-AAc) and EDA-functionalized poly(ACN-*co*-AAc), with R^2 values of 0.9930 and 0.9906, respectively. This suggests that the chemisorption process is more favourable for the adsorption of diclofenac when using both types of adsorbents.

Keywords: Diclofenac; ethanolamine-functionalized poly(ACN-*co*-AAc); ethylenediamine- functionalized poly(ACN-*co*-AAc); isotherm; kinetic; poly(acrylonitrile-*co*-acrylic acid)

ABSTRAK

Dalam kajian ini, sintesis poli(akrilonitril) (PAN) dan poli(akrilonitril-*ko*-asid akrilik) (poli(ACN-*ko*-AAc)) telah dijalankan melalui pempolimeran redoks dengan menggunakan natrium bisulfat (SBS) dan kalium persulfat (KPS) sebagai pemula. Kemudian, poli(ACN-*ko*-AAc) yang terhasil telah difungsikan dengan etanolamina (ETA) dan etilendiamina (EDA) untuk digunakan sebagai penjerap bagi penyingkiran diklofenak daripada larutan akueus. Sifat poli (ACN-*ko*-AAc) yang tidak difungsikan dan yang telah difungsikan telah dikaji menggunakan spektroskopi inframerah transformasi Fourier (FTIR), Mikroskop Elektron Imbasan (SEM), Analisis Termogravimetrik (TGA) dan analisis Brunauer-Emmett-Teller (BET). Semasa proses penjerapan, kami telah mengkaji kesan pH, kepekatan awal larutan diklofenak, masa sentuhan dan dos penjerap. Data isoterma paling sesuai dengan model Langmuir yang menunjukkan mekanisme penjerapan berlapis tunggal. Kapasiti penjerapan maksimum yang diperoleh daripada persamaan Langmuir lebih tinggi untuk poli(ACN-*ko*-AAc) yang telah difungsikan dengan ETA, iaitu 120.5 mg/g,

berbanding dengan poli(ACN-*ko*-AAc) yang telah difungsikan dengan EDA, iaitu 80.6 mg/g. Selain itu, hasil kinetik uji kaji kami menunjukkan bahawa model pseudo-tertib-kedua berkesan untuk menggambarkan kadar penjerapan diklofenak menggunakan kedua-dua jenis penjerap, iaitu poli(ACN-*ko*-AAc) yang telah difungsikan dengan ETA dan EDA, dengan nilai R^2 masing-masing sebanyak 0.9930 dan 0.9906. Ini menunjukkan bahawa proses kimia penjerapan lebih baik untuk penjerapan diklofenak apabila menggunakan kedua-dua jenis penjerap ini.

Kata kunci: Diklofenak; EDA-difungsikan poli(ACN-*ko*-AAc); ETA-difungsikan poli(ACN-*ko*-AAc); isoterma; kinetik; poli(ACN-*ko*-AAc)

Introduction

Pharmaceuticals are responsible for increasing life expectancy; as their consumption increase, they are now more frequently disposed of and detected in natural waters as emerging contaminants (Alessandretti et al. 2021). Improperly discarding unused pharmaceutical products is becoming an increasingly significant issue worldwide currently (Mohammed, Kahissay & Hailu 2021). Diclofenac (DCF) is a popularly prescribed anti-inflammatory drug due to high effectiveness in the alleviating pain and physical disability especially in rheumatic diseases. As a result, it has become one of the top-selling drugs in the market (Lonappan et al. 2016). However, among the various pharmaceuticals, diclofenac is becoming a major issue as it is commonly found in the aquatic environment (Khan & Anwer 2020). In addition, environmental pollution is increasingly worse as the pharmaceutical sector develops (Guo, Qi & Liu 2017). Due to the environmental consequences DCF can cause, it has received great attention since the early 2000s (Bonnefille et al. 2018).

Diclofenac is an emergent environmental pollutant due to its widespread presence in freshwater ecosystems and potential toxicity toward many organisms (Lonappan et al. 2016). The environmental impact of diclofenac is evident from a notable decline in vulture populations in Pakistan and India. This decline can be attributed to renal failure in vultures caused by the ingestion of polluted water containing DCF (Yaghmaeian et al. 2022). Diclofenac has a low rate of biodegradation and a high rate of persistence in wastewater-treatment facilities, resulting in bioaccumulation in surface waters, sediments, and sludges. To diminish or remove its presence in effluents, it is required to adopt some treatments (Angosto, Roca & Fernández-López 2020).

To effectively remove diclofenac from wastewater, several variable removal techniques have been investigated in prior studies. These techniques include ozonation (Qiu et al. 2020), advanced oxidation (Angosto, Roca & Fernández-López 2020), photocatalytic (Lara-Pérez et al. 2020), ion exchange (Adelli et al. 2017), and adsorption (Jodeh et al. 2016). However, some of these methods require costly equipment and may even release by-products that resulted damage to the environment and humans. Regarding wastewater treatment, adsorption is considered as a more efficient, profitable cost, and the easiest method among other techniques in decreasing and eliminating hazardous contaminants (AL-Kindi et al. 2021).

Polyacrylonitrile (PAN) is an industrially useful polymer due to its distinctive and well-known characteristics. Nevertheless, PAN has its weakness as it lacks the functionality to act as an adsorbent to capture diclofenac. PAN's low moisture absorption, hydrophobicity, and lack of active activity were caused by the strong nitrile dipolar interaction (Zahri et al. 2015). To improve PAN's performances, acidic *co*-monomers are introduced during the polymerization of PAN such as acrylic acid (AAc) to produce poly(acrylonitrile-*co*-acrylic acid) (poly(ACN-*co*-AAc)). Poly(ACN-*co*-AAc) has improved properties compared to PAN due to the addition of an acrylic acid monomer. This addition decreased its hydrophobicity and enhances the interaction between the carboxylic group and the nitrile group during the cyclization step (Rapeia et al. 2015).

In this study, redox copolymerization process was employed to synthesize poly(ACN-*co*-AAc) by reacting acrylonitrile monomer with acrylic acid. The incorporation of acrylic acid into the copolymer was aimed to enhance the hydrophobicity of PAN, which, in turn, would facilitate its chemical modification with amine-based reagents. Redox polymerization was chosen due to its advantages, including lower solvent consumption, shorter reaction time, higher polymer yield, and fewer side reactions, making it particularly suitable for use at lower temperatures (Göktaş 2020).

Poly(ACN-*co*-AAc) was further chemically functionalized with ethanolamine (ETA) and ethylenediamine (EDA). Polymers that have been chemically modified with amines (Liang et al. 2019), thiourea (Zhu et al. 2020), or amino acids (Chu et al. 2019) are expected to have better interaction with the active functional groups present in emerging contaminants. In this study, carboxyl and amine groups serve as the two functional groups that are responsible to build electrostatic interaction with both organic and inorganic pollutants in aqueous solutions (Adeyi et al. 2019). The polymer underwent chemical functionalization to produce polymeric materials with specific properties tailored for an adsorption process. Surface alterations, either physical or chemical, are essential for enhancing the adsorbent's performance (Rapeia et al. 2015). In this work, the effects of different types of amine-functionalized poly(ACN-*co*-AAc) as an adsorbents to capture diclofenac from an aqueous solution were compared. Isotherm and kinetics studies were also conducted to further examine the process. The chemical modification reaction of poly(ACN-*co*-AAc) with ETA and EDA is illustrated in Scheme 1. In ETA-functionalized poly(ACN-*co*-AAc), the presence of -OH, -NH-R groups, which consist of lone pair electrons is expected to establish electrostatic interaction with diclofenac, the target analyte in this study. On the other hand, the presence of -NH-R and -NH_2 groups in EDA-functionalized poly(ACN-*co*-AAc) are also expected to facilitate electrostatic interaction with diclofenac. Two types of modification agents, ETA and EDA, were used to compare their performance during the adsorption process. The utilization of modified poly(ACN-*co*-AAc) with ETA and EDA for the adsorption of diclofenac from an aqueous solution has never been reported before. The aims for this research are to chemically modify poly(ACN-*co*-AAc) with amine functional groups, namely ethanolamine (ETA) and ethylenediamine (EDA), and also to investigate the adsorption capacity of diclofenac onto amine-modified poly(ACN-*co*-AAc) copolymers in an aqueous solution. These aims emphasize the novel approach of employing amine-modified copolymers for the adsorption of diclofenac in aqueous environment, filling a gap in existing literature.

Methods

Materials

The reagent used for the synthesis of the polymer were acrylonitrile (MERCK, Darmstadt, Germany) and acrylic acid (R&M Chemicals, UK). Monomers were purified by using aluminium oxide (MERCK, Darmstadt, Germany) to remove the impurities. The initiators used in the polymerization were sodium bisulphate (SBS) (R&M Chemicals, UK) and potassium persulfate (KPS) (Sigma-Aldrich, Dorset, UK). Deionized water was used as the reaction medium. For chemical functionalization of poly(ACN-*co*-AAc), the reagents used were ethanolamine (ETA) and ethylenediamine (EDA) which were supplied by Sigma-Aldrich, Dorset, UK. Methanol and acetone

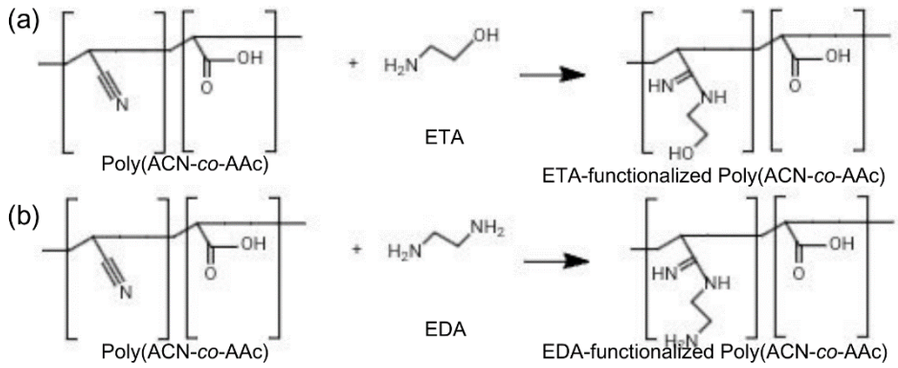

SCHEME 1. Chemical modification of poly(ACN-*co*-AAc) with (a) ethanolamine (ETA) and (b) ethylenediamine (EDA

were purchased from R&M Chemicals, UK. Sodium hydroxide (R&M Chemicals, UK) and hydrochloric acid (R&M Chemicals, UK) were used to adjust the pH during adsorption studies. Sodium chloride was purchased from Sigma-Aldrich, Dorset, UK. It was used for the determination of the pH_{PZC} of the adsorbents. Diclofenac (Friendemann Schmidt SDN BHD) was used as an organic pollutant for adsorption study.

SYNTHESIS OF PAN

The redox polymerization was carried out in a three-necked round bottom flask, fitted with a water condenser, and maintained at a temperature of 40 °C under a continuous flow of N_2 gas. To ensure the purity of acrylonitrile (ACN), it was passed through a column of neutral aluminum oxide (Al_2O_3). The reaction medium, consisting of 200 mL of deionized water, was purged with N_2 gas for 30 min then it was added with 20 mL of purified ACN, 2.09 g of SBS, and 2.15 g of KPS. The mixture was mechanically stirred at a speed of 200 rpm, and the polymerization process was allowed for 3 h. After the synthesis reaction was completed, the polymer slurry was added to 20 mL of methanol and was allowed to precipitate for 1 h. The precipitated polymer was then filtered and washed with 50 mL of methanol followed by 100 mL of deionized water. The polymer was dried in a vacuum oven at 45 °C until a constant weight was obtained. This polymerization method is according to the synthesis method that was reported by Zahri et al. (2015).

SYNTHESIS OF POLY(ACN-co-AAc)

Redox polymerizations of poly(ACN-*co*-AAc) were carried out at 40 °C under N_2 gas with a similar apparatus set-up earlier. The ACN and acrylic acid (AAc) were purified by passing them through a short column of neutral aluminium oxide (Al_2O_3). Feed ratios of ACN: AAc was 95:5. The copolymerization employed 18 mL of AN and 2 mL of AA as reaction feed. N_2 gas was used to purge the reaction medium (200 mL deionized water) for 30 min. The reaction medium was added with 18 mL of purified ACN, 2 mL of purified AAc, 2.09 g of SBS, and 2.15 g of KPS. The mixture was mechanically stirred at 200 rpm. The polymerization process was conducted for 3 h. After completion of polymerization, the copolymer was precipitated in methanol for 1 h. The precipitated polymer was then filtered and washed with 50 mL of methanol followed by 100 mL of deionized water. The polymer was dried in a vacuum oven at 45 °C until a constant weight was obtained. A similar method was reported by Zahri et al. (2015).

CHEMICAL FUNCTIONALIZATION OF POLY(ACN-co-AAc)

100 mL solution of 1.0 M ethanolamine (ETA) was added to a round-bottomed flask. 0.500 g of poly(ACN-*co*-AAc) was added to the flask and the mixtures were allowed to react for 4 h at 70 ºC and stirred at 80 rpm. After completion of the reaction, the poly(ACN-*co*-AAc) was filtered and washed with 20 mL of methanol, 20 mL of acetone, and 20 mL of deionized water. The chemically functionalized polymer was dried at 60 °C in a vacuum oven. The same method was again applied in the modification of poly(ACN-*co*-AAc) using ethylenediamine (EDA).

CHARACTERIZATION

Fourier transform infrared (FTIR) analysis was performed using a Spectrum 100 Perkin Elmer (U.S.A) instrument equipped with Universal Attenuated Total Reflectance (UTAR) and potassium bromide (KBr) pellets. The analysis covered a resolution range of 4000–500 cm^{-1} and was carried out at room temperature. A Perkin Elmer (STA6000,U.S.A) instrument was employed under a nitrogen atmosphere to study thermogravimetric analysis (TGA). The temperature range studied was from 50 to 1000 °C at a heating rate of 10 °C·min^{-1}. Scanning electron microscopy (SEM) was conducted using a JEOL JSM 6360 LA instrument from Japan, operating at 10.0 to 25.0 kV. Brunauer-Emmett-Teller (BET) analysis was carried out by using Micrometrics ASAP 2010 (U.S.A.) surface area analyser. The samples were degassed overnight at 100 °C under vacuum before being analysed using nitrogen sorption at 77 K.

DETERMINATION OF THE POINT OF ZERO CHARGES (pH_{PZC}) OF EACH ADSORBENT

50 mL of 0.001 M NaCl were initially added to eight 250 mL Erlenmeyer flasks, respectively. The initial pH was adjusted between the range of 2 and 9 at one-point intervals. 0.1 M HCl and 0.1 M NaOH were used to control the pH. 0.010 g of the poly(ACN-*co*-AAc) was immediately added to the flask after achieving a steady $pH_{initial}$ value. To achieve equilibrium, the solutions were stirred for 24 h. The pH of the solution was tested after 24 h and recorded as pH_{final}. The pH_{PZC} of poly(ACN-*co*-AAc) is the point when $pH_{initial} = pH_{final}$ (Park et al. 2012). The

same method was again applied for ETA-functionalized poly(ACN-*co*-AAc) and EDA-functionalized poly(ACN-*co*-AAc).

ADSORPTION OF DICLOFENAC USING AMINE-FUNCTIONALIZED POLY(ACN-co-AAc)

10 mg of amine-functionalized poly(ACN-*co*-AAc) was added to 20 mL of 20 ppm of a diclofenac in a centrifuge tube. The mixture of the solution was allowed to reach equilibrium overnight before analysis. The solution was centrifuged at room temperature (25 °C) for 10 min at a speed of 4,000 rpm. A 3.00 mL sample of the resulting supernatant was taken and passed through a 0.2 µm Millipore filter syringe to eliminate any remaining particles in solution. The percentage removal of pharmaceuticals can be expressed as Equation (1):

$$\text{Percentage removal (\%)} = \left(\frac{C_o - C_e}{C_o}\right) \times 100\ \% \qquad (1)$$

where C_o is the initial concentration(mg/L) and C_e is the equilibrium adsorbate concentration (mg/L).

ADSORPTION ISOTHERM

10 mg of amine-functionalized poly(ACN-*co*-AAc) adsorbent with different initial concentration of diclofenac (20-120 mg/L) was used to determine the adsorption isotherms. The adsorption capacity was determined using Equation (2):

$$q_e = \left(\frac{C_o - C_e}{m}\right) \times v \qquad (2)$$

where q_e (mg/g) denotes the quantity of adsorbate being adsorbed on per gram of adsorbent at equilibrium. C_o and C_e represent the initial and equilibrium concentration in solution (mg/L), respectively. m (g) indicates the quantity of adsorbent used and v (L) is the volume of the solution. A graph of $1/q_e$ versus $1/C_e$ for the Langmuir isotherm model and a graph of log q_e versus log C_e for the Freundlich isotherm model was plotted to analyse the data.

ADSORPTION KINETICS

The adsorption kinetics of the adsorbent was studied by varying the contact time (1, 3, 5, 10, 15, 20, 25, 30, 45, 60 min) of amine-functionalized poly(ACN-*co*-AAc) (10 mg) with diclofenac. Equation 3 was used to calculate the amount of polar solvent adsorbed by the adsorbent at the time (*t*):

$$q_t = \left(\frac{Co - Ct}{m}\right) \times v \qquad (3)$$

in which q_t (mg/g) denotes the quantity of adsorbate adsorbed on per gram of the adsorbent at time t. C_o and C_t represent the initial concentration and adsorbate concentration at time (*t)* in solution (mg/L), respectively; m (g) indicates the quantity of adsorbent; and (L) is the volume of the solution. A graph of log (q_e-q_t) versus time for the pseudo-first-order model and a graph of t/q_t versus time for the pseudo-second-order model was plotted to analyse the obtained data.

RESULTS AND DISCUSSION

YIELDS OF POLYMERIZATION

Table 1 presents the percentage yield of PAN and poly(ACN-*co*-AAc) that has been obtained, which are 96% and 94%, respectively. As expected, copolymer yield percentages are lower than PAN yield percentages. PAN has a higher percentage yield due to non-incorporation with other monomers during polymerization that disturbed the chain reaction (Jamil, Daik & Ahmad 2010). The AAc monomer that contains the -COOH functional group was inadequate in building polymer chains, which lead to producing a low yield in poly(ACN-*co*-AAc) (Rapeia et al. 2015).

TABLE 1. Percentage yield of polymers

Samples	ACN/AAc (mol%)	Percentage yield (%)
PAN	100/0	96%
Poly(ACN-*co*-AAc)	95/5	94%

FOURIER TRANSFORM INFRARED (FTIR) ANALYSIS

The FTIR method was used to detect functional groups in polymer chains. The FTIR spectra were recorded in the range of 500–4000 cm^{-1} using an FTIR instrument. Figure 1 illustrates the IR spectra for PAN, poly(ACN-*co*-AAc), ETA-functionalized poly(ACN-*co*-AAc) and EDA-functionalized poly(ACN-*co*-AAc). In the IR spectrum of PAN, an absorption band at 2243 cm^{-1} indicated the presence of the nitrile group (C≡N). Additionally, another band at 2938 cm^{-1} suggested the presence of C-H stretching in PAN. The IR spectrum of unfunctionalized poly(ACN-*co*-AAc) showed a prominent band at 1734 cm^{-1}, which can be attributed to the C=O group, confirming the successful copolymerization of AAc

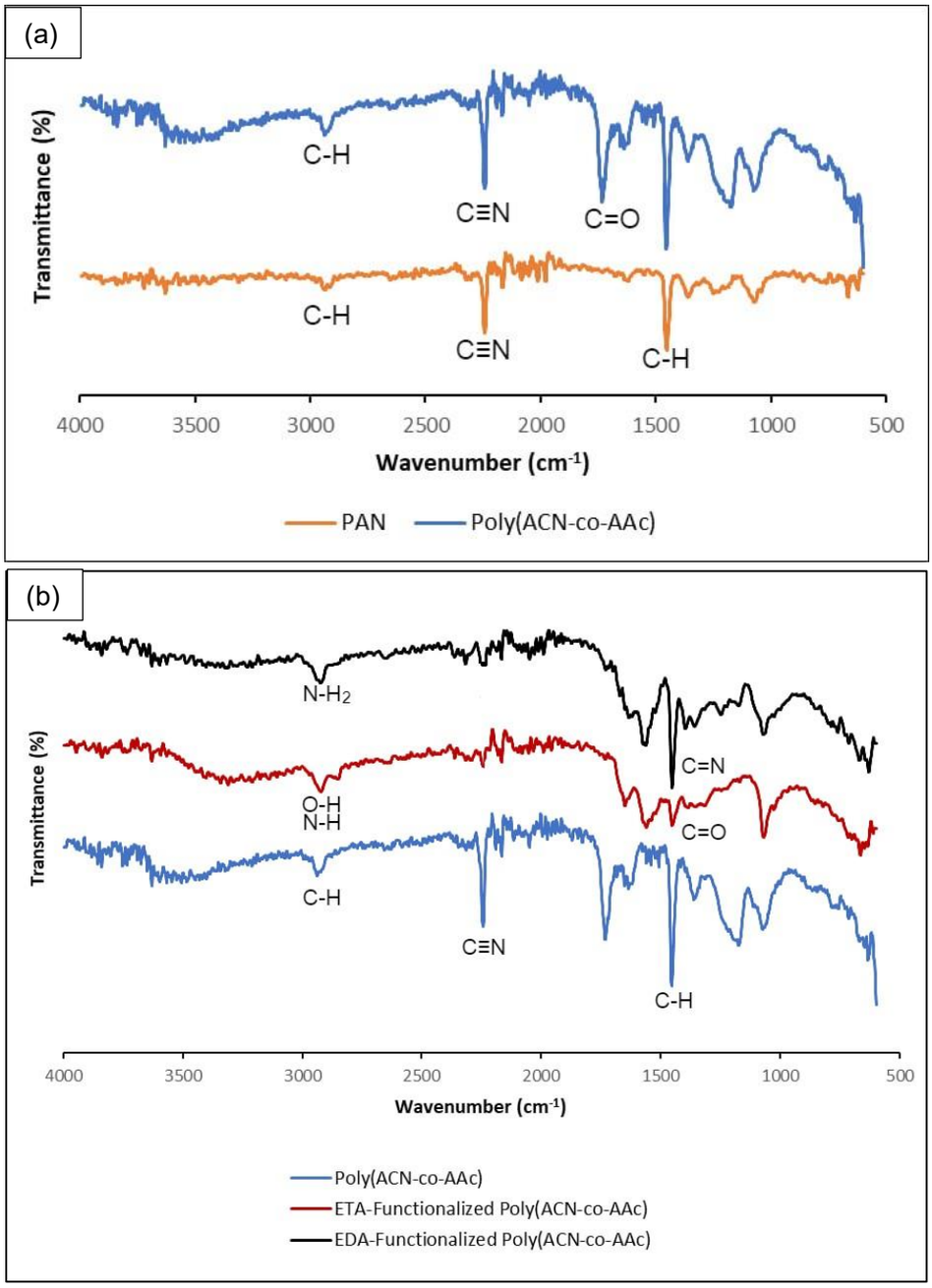

FIGURE 1. (a) IR spectra for PAN and poly(ACN-co-AAc), and (b) IR spectra for poly(ACN-co-AAc), ETA-functionalized poly(ACN-*co*-AAc) and EDA-functionalized poly(ACN-*co*-AAc)

with ACN to produce poly(ACN-*co*-AAc) (Zahri et al. 2015). For ETA-functionalized poly(ACN-*co*-AAc), the absorption of the OH group in the presence at 3270 cm^{-1} overlapped with N-H stretching bands. The absorption bands were observed at the region 3246 cm^{-1} indicating the presence of the N-H_2 group in ethylenediamine for poly(ACN-*co*-AAc) functionalized with EDA. The nitrile group (C≡N) in both spectra of functionalized poly(ACN-*co*-AAc) disappeared, indicating the conversion of the nitrile group into an amine group in the functionalized chemical structure. In addition, new absorption bands appeared in the range of 1643–1629 cm^{-1} that were assigned to the C=N stretching which overlapped with C=O stretching. This observation confirms the successful of chemical functionalization for both amine-functionalized poly(ACN-*co*-AAc).

POINT OF ZERO CHARGE

The point of zero charges (pH_{PZC}) is measured when pH has an equal charge of the positive and negative surface sites, or when the adsorbent surface charge is zero. At pH<pH_{PZC}, the surface charge is positive while at pH>pH_{PZC}, the surface charge is expected to be negative (Kołodziejska & Kołodziejczyk 2018). Figure 2 shows that the obtained values of pH_{PZC} of poly(ACN-*co*-AAc), ETA-functionalized poly(ACN-*co*-AAc), EDA-functionalized poly(ACN-*co*-AAc) are close to neutrality which are 7.12, 6.82, and 6.53, respectively. The unmodified polymer's surface is electrically neutral when the pH of the surrounding solution is around 7.12. In other words, it exhibits neither a net positive nor a net negative charge at this pH. The functionalization with ETA has slightly shifted the pH_{PZC} towards acidity compared to the unmodified polymer. This change can affect the polymer's adsorption properties and reactivity, making it more favorable in slightly acidic conditions (Christian et al. 2017). EDA-functionalized poly(ACN-*co*-AAc) shows a similar trend as ETA-functionalized polymer. The pH_{PZC} values for these polymers and their functionalized forms indicate how the surface charge of the materials changes as a result of chemical modification.

THERMOGRAVIMETRIC ANALYSIS (TGA)

Figure 3(a) and (b) shows the thermal analysis curves for PAN, poly(ACN-*co*-AAc), ETA-functionalized poly(ACN-*co*-AAc), and EDA-functionalized poly(ACN-*co*-AAc), respectively. The thermogram in Figure 3(a) showed the char yield of the respective adsorbent at 900 °C. It shows that the char yield of poly(ACN-*co*-AAc) is the highest (22.91%), followed by PAN (16.96%). Poly(AACN-*co*-AAc) has a higher char yield as compared to that of PAN, due to the inclusion of an AAc repeating

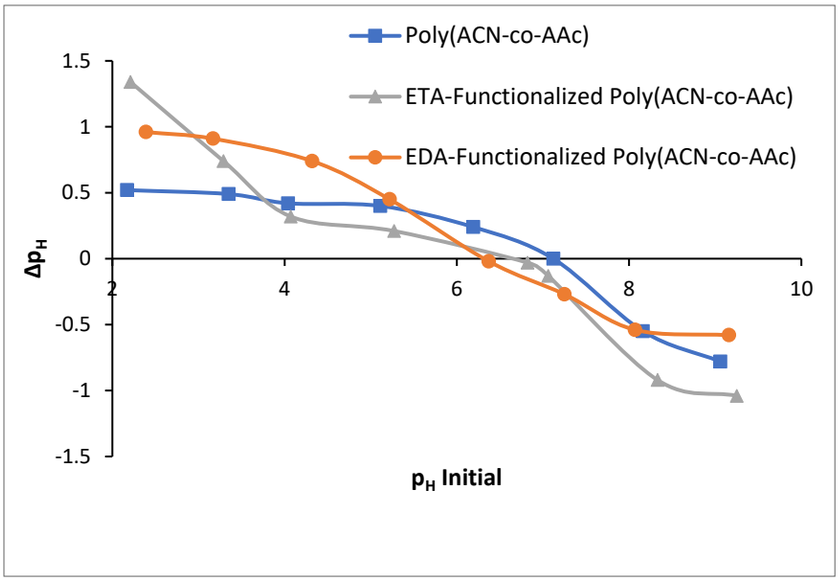

FIGURE 2. Determination of pH_{PZC} for each adsorbent

unit in the copolymer system that inhibited the nitrile-nitrile cyclization process, hence lowering the exothermic process. Meanwhile, in the case of PAN, the cyclization process occurred at a higher rate and causes more fragmentation of chains as compared to that of poly(ACN-*co*-AAc). This causes a lower char yield of PAN as compared to that of its copolymer. The observations can be explained by the DTG curves of respective adsorbents. As shown in Figure 3(b), PAN shows a more intense peak at 300 °C as compared to that of poly(ACN-*co*-AAc). The presence of acrylic acid (AAc) in polyacrylonitrile (PAN) molecules impacts the arrangement of nitrile-nitrile atoms within the poly(ACN-*co*-AAc) chain which was affecting the cyclization process. These changes were attributed to intra or intermolecular interactions between AAc and ACN monomer (Zahri et al. 2015). As a result, the cyclization rate of poly(ACN-*co*-AAc) was lower compared to PAN. Cyclization of nitrile-nitrile groups in PAN is associated with the release of heat during the stabilization process. Cyclization of PAN involves a free radical mechanism, whereas copolymer of ACN and AAc undergoes cyclization via an ionic mechanism, in which the heat evolvement is lesser as compared to that of the free radical mechanism (Park et al. 2012).

The amine-functionalized copolymer has a lower char yield at 6.89% (ETA-functionalized poly(ACN-*co*-AAc)) and 0% for the EDA-functionalized poly(ACN-*co*-AAc). This might be due to the conversion of nitrile groups along the chains into extended imine groups and affects the copolymer thermal stability (Adeyi et al. 2019). The absence of nitrile groups reduced the thermal stability of amine-functionalized poly(ACN-*co*-AAc) hence, resulted in low char yield at 900 °C. These can be explained by the DTG curves of poly(ACN-*co*-AAc) that showed two DTG curves due to the presence of two monomers in the copolymer composition which were ACN and AAc at 256 °C and 430 °C, respectively. However, the DTG curve of unfunctionalized poly (ACN-*co*-AAc) has less curve compared to ETA- functionalized poly(ACN-*co*-AAc) has 4 small DTG curve peaks while EDA- functionalized poly(ACN-*co*-AAc) has two small curve and one broad curve appearing in the range between 250 °C - 450 °C. This indicates the existence of ETA and EDA in copolymer chains. The differences in DTG curves between (poly(ACN-*co*-AAc)) and modified poly(ACN-*co*-AAc) can be attributed to the effects of chemical modification. These modifications can introduce new chemical bonds, which may result in increased thermal stability and a simpler degradation. Functionalization can lead to a more uniform degradation process by enhancing intermolecular interactions compared to unmodified polymer. The residue weights of ETA-functionalized poly (ACN-*co*-AAc) and EDA-functionalized poly (ACN-*co*-AAc) were negatives indicate that some chemical reactions or interactions have occurred during the functionalization process that have resulted in a loss of mass or other changes in the polymer structure.

SCANNING ELECTRON MICROSCOPY (SEM) ANALYSIS

Figure 4(a)-4(d) shows the surface morphology of PAN, poly(ACN-*co*-AAc), ETA-functionalized poly(ACN-*co*-AAc), and EDA-functionalized poly(ACN-*co*-AAc), respectively. The spherical particles in Figure 4(a) show that PAN has an agglomerated shape of small particles and a coarse surface. Particles of poly(ACN-*co*-AAc) and amine-functionalized poly(ACN-*co*-AAc) appeared spherical, agglomerated, and have a rough surface. According to Adeyi et al. (2019), the agglomeration and spherical shape of the ACN-AAc monomers were influenced by factors such as water content (lower viscosity), type of initiator, and intraparticle bonding. Furthermore, the rates of adsorption were found to be higher on rough surfaces compared to smooth surfaces. It is expected that the rougher adsorbent's surface provides larger surface area (Venkatakrishnan & Kuppa 2018).

The average sizes of particles of PAN were higher than poly(ACN-*co*-AAc) which was 163 nm. The solvation of the reaction medium towards the polymer phase becomes poorer due to an increase in AA incorporation in the PAN system. As a result, early phase separation of the polymer from the monomer phase occurred, resulting in a decrease in the particle size of poly(ACN-*co*-AAc) (Zahri et al. 2015). Average size particles after the modification process slightly increased as compared to that poly(ACN-*co*-AAc) which were 289 nm for ETA-modified poly(ACN-*co*-AAc) and 271 nm for poly(ACN-*co*-AAc). These changes further confirmed the successful surface functionalization by the amine group towards poly(ACN-*co*-AAc) surface (Adeyi et al. 2019).

BRUNAUER-EMMETT-TELLER SURFACE AREA (BET) ANALYSIS

The surface area, pore volume, and pore size of PAN, poly(ACN-*co*-AAc) and amine-functionlized poly(ACN-*co*-AAc) are summarized in Table 2. The surface area of PAN was lower (2 m^2/g) as compared to that of poly(ACN-

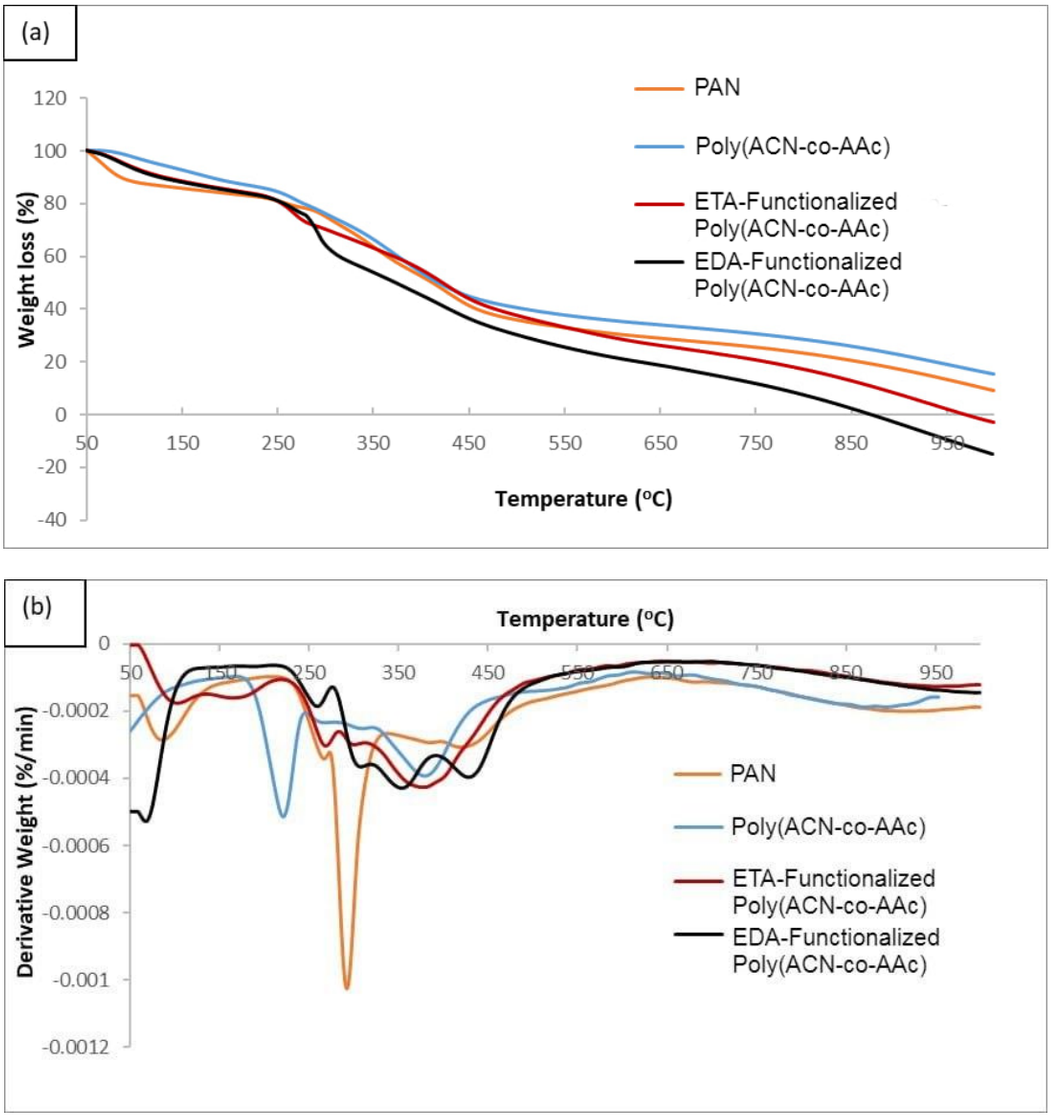

FIGURE 3. (a) TG curves and (b) DTG curves for PAN, poly(ACN-*co*-AAc), ETA-functionalized poly(ACN-*co*-AAc) and EDA-functionalized poly(ACN-*co*-AAc)

co-AAc) (23.61 m^2/g). This is probably due to the presence of AAc that reduced the polarity of PAN chains and thus facilitate the formation of pores of polymeric chains. As shown in Table 2, the chemical modification of poly(ACN-*co*-AAc) reduces the surface area of the copolymer from 23.61 m^2/g to 4.68 m^2/g for ETA-functionalized poly(ACN-*co*-AAc) and 15.06 m^2/g for ETA-functionalized poly(ACN-*co*-AAc), respectively. The mean pore size of the chemically functionalized copolymer was larger as compared to that of the copolymer. This might be due to the disruption of pore walls within polymeric structures that reduce the specific surface area, hence increasing the pores' size (Popa et al. 2020).

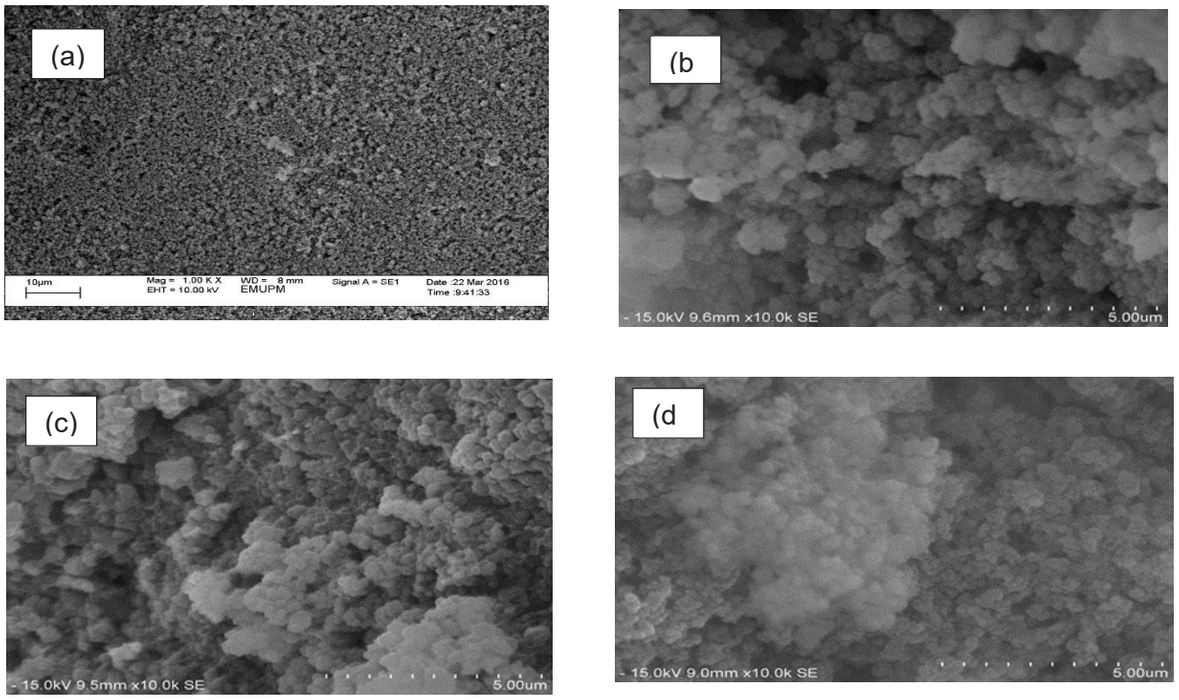

FIGURE 4. SEM images of (a) PAN, (b) Poly(ACN-*co*-AAc), (c) ETA-functionalized poly(ACN-*co*-AAc), and (d) EDA-functionalized poly(ACN-*co*-AAc)

TABLE 2. BET data for PAN, Poly(ACN-*co*-AAc), ETA-functionalized Poly(ACN-*co*-AAc), and EDA-functionalized Poly(ACN-*co*-AAc)

Samples	Specific surface area (m^2/g)	Specific pore volume (cm^3/g)	Mean pore size (nm)
PAN	2.00	-	-
Poly(ACN-*co*-AAc)	23.61	1.49	126
ETA-functionalized poly(ACN-*co*-AAc)	4.68	1.03	439
EDA-functionalized poly(ACN-*co*-AAc)	15.06	1.37	181

BATCH ADSORPTION OF DICLOFENAC

Effect of pH

Figure 5 shows the percentage removal of diclofenac and the adsorption capacity of diclofenac in the pH range between 3 and 11 for each adsorbents. Based on the results, it is observed that the optimal pH for a high % removal for all adsorbents was 7. The highest percentage removal of diclofenac by EDA-functionalized poly(ACN-*co*-AAc) was 83% (166.0 mg/g), followed by ETA-functionalized poly(ACN-*co*-AAc) and poly(ACN-*co*-AAc) which were 78% (156.5 mg/g) and 65% (130.5 mg/g), respectively.

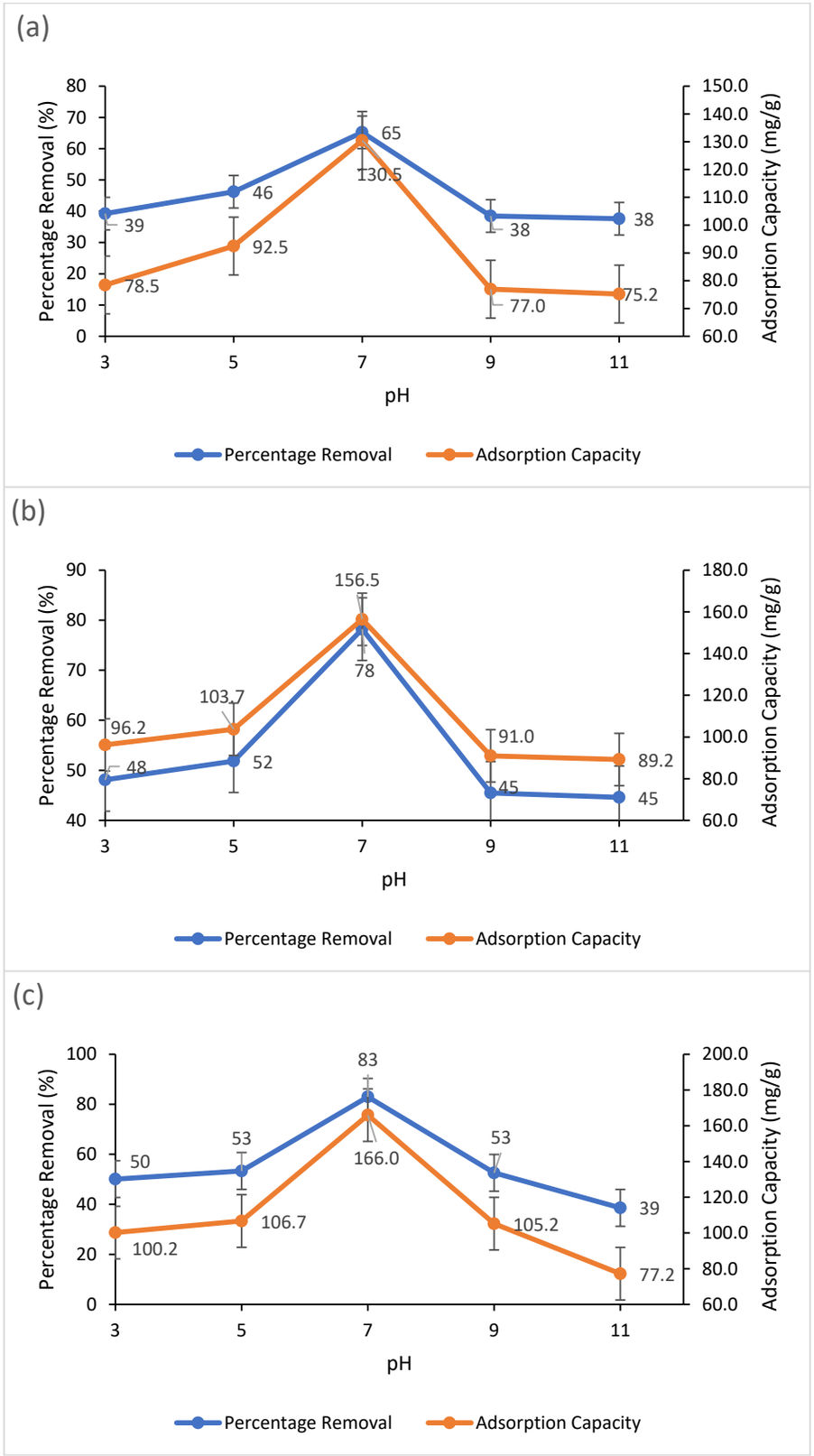

FIGURE 5. Effect of pH on the percentage removal and the adsorption capacity of diclofenac solution for (a) poly(ACN-*co*-AAc), (b) ETA-functionalized poly(ACN-*co*-AAc), and (c) EDA-functionalized poly(ACN-*co*-AAc)

The results show that the adsorption of diclofenac escalated as the solution pH increased from 3 to 7. This is probably because diclofenac is a weak acid with pKa value of 4.15, and it exhibits limited ionization at lower pH levels (Ghavi, Raouf & Koohi 2020). Therefore, as the pH of the surrounding increased, diclofenac experienced a higher ionization process, hence causing better adsorption on the surface of the less positively charged adsorbent. When the pH of the solution is below the pH_{PZC} value (approximately 7.00), the solid surface of the adsorbent develops a mainly positive net surface charge. Hence, the adsorption of diclofenac is favoured via coulombic attractions onto the surface that is dominated by H^+(Ghavi, Raouf & Koohi 2020).

On the other hand, when the pH of the solution exceeds pH 7, the adsorption uptake of diclofenac was significantly decreased. The reduced of the removal percentage of diclofenac caused by the excessive presence of hydroxyl (OH-) groups in the solution, which hinders the interaction between the adsorbent and diclofenac (Ghavi, Raouf & Koohi 2020). At higher pH levels, the basic nature of the solution leads to the deprotonation of hydroxyl groups on the surface of the adsorbent. Consequently, this deprotonation process can lead in repulsion between the negatively charged adsorbent surface and diclofenac molecules (Leone et al. 2017).

Effect of Adsorbent Dosage

Figure 6 shows the influence of adsorbent dosage on the extent of removal and adsorption capacity for DCF for each adsorbent, respectively. The diclofenac uptake increased by increasing the dosage for each type of adsorbent from 10 mg to 50 mg. The percentage removal was increased up to 89% for EDA- functionalized poly(ACN-*co*-AAc), 84% for ETA-functionalized poly(ACN-*co*-AAc) and 65% for poly(ACN-*co*-AAc) at 50 mg, respectively. At low adsorbent dosages, the efficiency of DCF ion removal by the adsorbent is decreased due to a mismatch between the available binding sites and the adsorbent's holding capacity. However, with an increase in adsorbent dosage, the adsorption capacity increase with larger number of DCF ions are captured by the remaining unsaturated surface centers (Yusuff 2019). Adsorption capacity also increased as the adsorbent dosage increased. As shown in Figure 6, the maximum adsorption capacity for poly(ACN-*co*-AAc), ETA-functionalized poly(ACN-*co*-AAc) and EDA-functionalized poly(ACN-*co*-AAc) were 129.2 mg/g, 168.5 mg/g, and 177.5 mg/g, respectively. Increasing adsorbent dosage produces more available adsorption sites which leads to an increase of adsorption capacity (Jodeh et al. 2016).

Effect of Contact Time

Figure 7 shows the effect of contact time on the percentage removal and adsorption capacity of diclofenac for poly(ACN-*co*-AAc, ETA-functionalized poly(ACN-*co*-AAc), and EDA-functionalized poly(ACN-*co*-AAc), respectively. In the case of poly(ACN-*co*-AAc), it was observed that both the percentage removal and adsorption capacity increased with prolonged contact time until reaching its equilibrium which was 70% and 140.6 mg/g at 30 min. The optimum contact time for ETA-functionalized poly(ACN-*co*-AAc) was also at 30 min with 87% (173.3 mg/g) of DCF uptake. Meanwhile, for EDA-functionalized poly(ACN-*co*-AAc), the adsorption of DCF reached its equilibrium at 25 min, a bit faster than copolymer and ETA-functionalized poly(ACN-*co*-AAc) with 90% of DCF removal and the maximum capacity of 180.2 mg/g. When the adsorbents reach saturation with DCF ions, the active binding sites slowly start to release the drug ions back into the solution. It means that additional time does not lead to an increase in the quantity of diclofenac that can be adsorbed (Kurniawati et al. 2021).

Effect of Initial Concentration

As shown in Figure 8, in the case of EDA-functionalized poly(ACN-*co*-AAc), the percentage removal increased as the initial concentration of diclofenac increased until its achieved equilibrium at 80 ppm with 96% of removal. Meanwhile, for unfunctionalized copolymer and ETA-functionalized poly(ACN-*co*-AAc), the percentage removal increased to 100 ppm, in which the maximum percentage removal is 70% and 90%, respectively. As expected, the functionalized copolymer has better adsorption towards diclofenac as compared to that of non-functionalized copolymer due to the existence of N and O atoms in the adsorbent's chain that potentially form electrostatic interaction with diclofenac. EDA-functionalized poly(ACN-*co*-AAc) resulted in the highest adsorption, and this might be due to the electrostatic interactions with the diclofenac ions by higher numbers of protonated amine groups of the adsorbents as compared to that of ETA- functionalized poly(ACN-*co*-AAc) (Aoopngan et al. 2019). At higher concentrations, the removal efficiency of DCF increased due to a larger presence of residual diclofenac ions in the aqueous solution. This induced to enhanced molecular interactions, resulting in bettered adsorption onto adsorbent's surface (Gorzin & Abadi 2017).

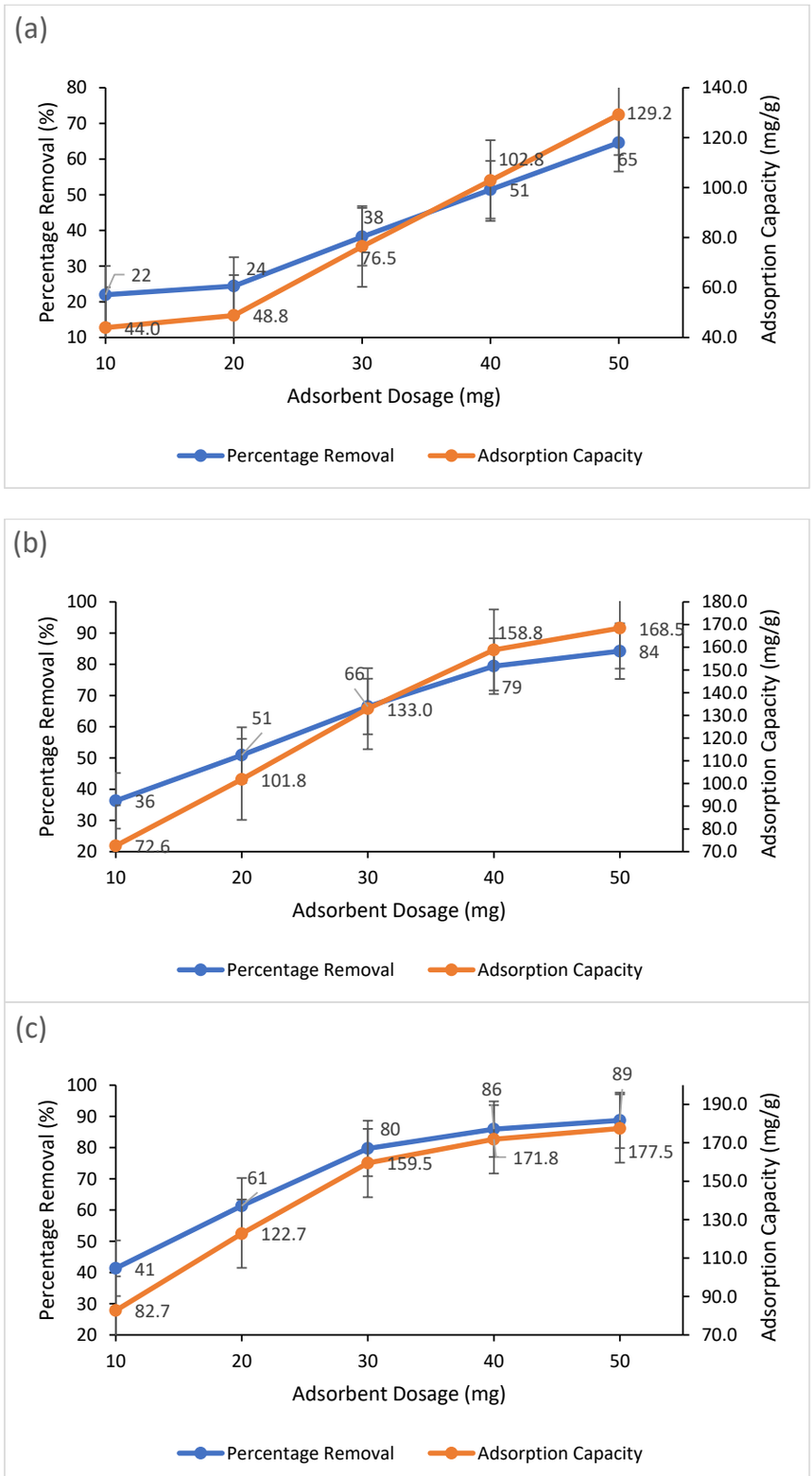

FIGURE 6. Effect of adsorbent dosage on the percentage removal and the adsorption capacity of diclofenac solution for (a) poly(ACN-*co*-AAc), (b) ETA-functionalized poly(ACN-*co*-AAc), and (c) EDA-functionalized poly(ACN-*co*-AAc)

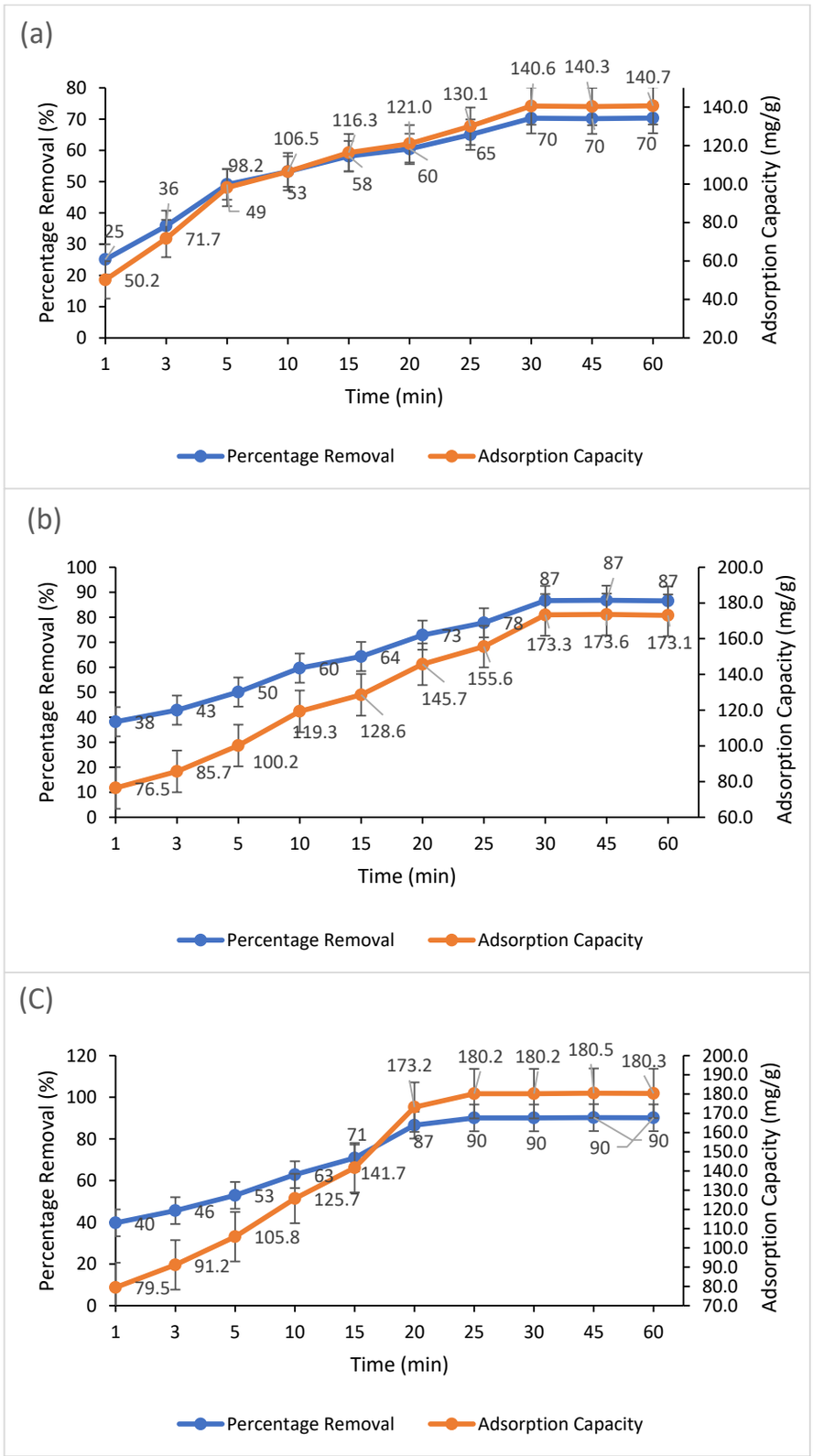

FIGURE 7. Effect of contact time on the percentage removal and the adsorption capacity of diclofenac solution for (a) poly(ACN-*co*-AAc), (b) ETA-functionalized poly(ACN-*co*-AAc), and (c) EDA-functionalized poly(ACN-*co*-AAc)

Figure 8 also shows the effect of the initial concentration of diclofenac on the adsorption capacity of the diclofenac. It was observed that the adsorption capacity increased as the initial concentration increased for each adsorbent. The maximum adsorption capacity was achieved at 120 ppm with 169.8 mg/g of diclofenac uptake for poly(ACN-*co*-AAc), 176.7 mg/g for ETA-functionalized poly(ACN-*co*-AAc), and 191.9 mg/g for EDA-functionalized poly(ACN-*co*-AAc), respectively. The higher initial concentrations of diclofenac ions in the solution result in the active sites on the surface of the adsorbent being surrounded by an increased amount of diclofenac ions. Consequently, this leads to a greater equilibrium adsorption capacity, thereby enhancing the overall adsorption process (Gorzin & Abadi 2017).

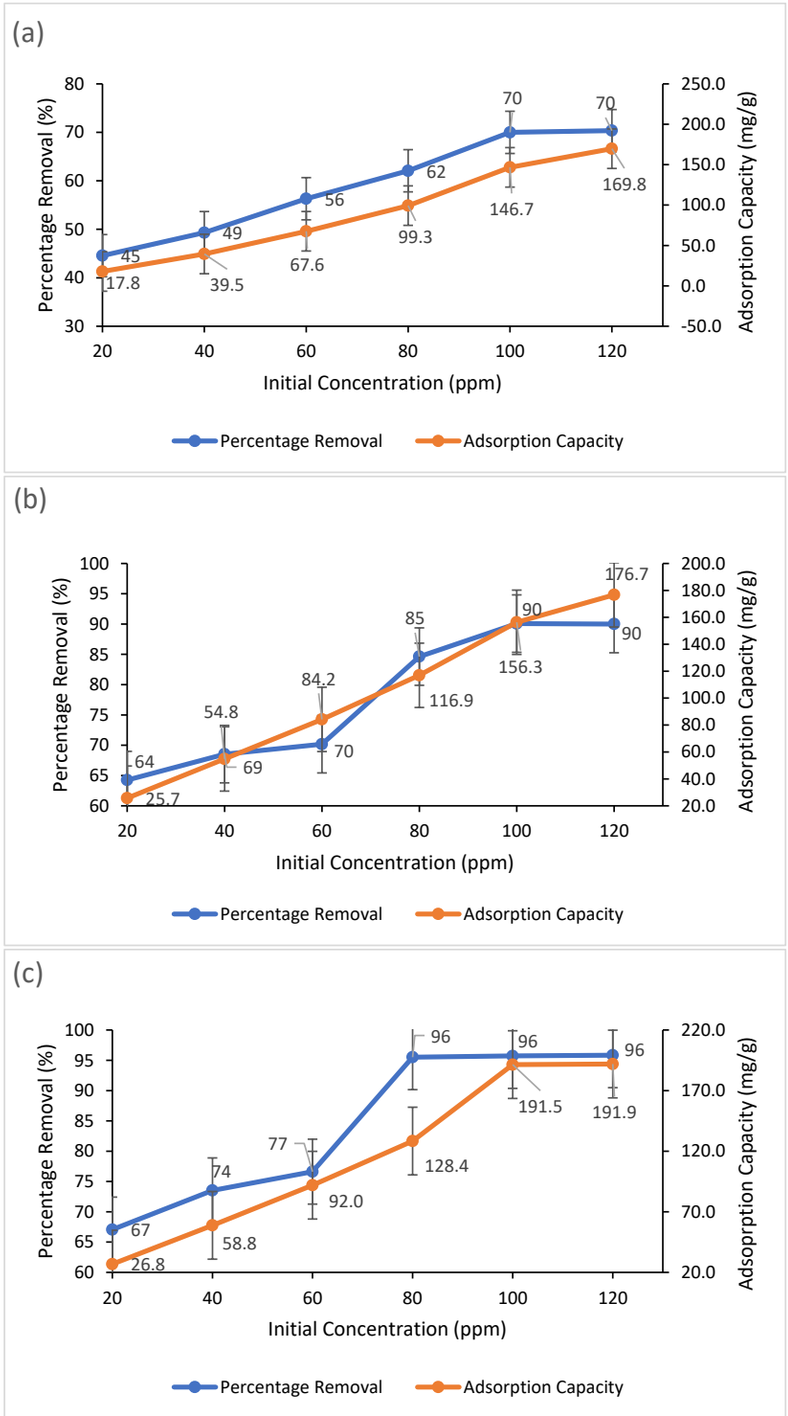

FIGURE 8. Effect of initial concentration on the percentage removal and the adsorption capacity of diclofenac solution for (a) poly(ACN-*co*-AAc), (b) ETA-functionalized poly(ACN-*co*-AAc), and (c) EDA-functionalized poly(ACN-*co*-AAc)

ADSORPTION ISOTHERM

In this research, Langmuir and Freundlich isotherm models are chosen for investigating the adsorption of isotherms onto diclofenac aqueous solutions. The linearised form of the Langmuir model can be expressed as:

$$\frac{1}{q_e} = \frac{1}{C_e}\frac{1}{K_L.q_m} + \frac{1}{q_m} \quad (4)$$

where K_L is the Langmuir constant (L mg^{-1}); q_m is the maximum mass of drugs adsorbed per unit mass of adsorbent for the formation of a complete monolayer on the surface of adsorbent (mg g^{-1}); C_e is the equilibrium concentration of drugs (mg L^{-1}); and q_e is the mass of drugs per unit mass of adsorbent at equilibrium (mg g^{-1}).

Adsorption processes that occur on heterogeneous surfaces can be explained by the Freundlich isotherm (Ayawei, Ebelegi & Wankasi 2017). The linear form of this isotherm is expressed as follows:

$$\log q_e = \frac{1}{n}\log C_e + \log K_F \quad (5)$$

where K_F is the distribution coefficient; and n is a correction factor. By plotting the linear form which is $\log q_e = 1/n \log C_e + \log K_F$, the parameters K_F and n can determine since the slope is $1/n$ and the intercept is equal to $\log K_F$.

Table 3 shows the isotherm parameters of diclofenac onto three different adsorbents. The Langmuir model has a higher value of the correlation coefficient which was 0.9938 for poly(ACN-*co*-AAc), 0.9925 for ETA-functionalized poly(ACN-*co*-AAc) and 0.9939 for EDA-functionalized poly(ACN-*co*-AAc), respectively, compared to the Freundlich model. The R^2 value is closer to 1.000 showing that the three adsorbents are fitted well into the Langmuir model, indicating the adsorption mechanism to be mono layered (Sathishkumar et al. 2015). The maximum adsorption capacities obtained from the Langmuir equation for ETA- functionalized poly(ACN-*co*-AAc) was 120.482 mg/g, which was higher compared to EDA-functionalized poly(ACN-*co*-AAc) and poly(ACN-*co*-AAc), with 80.645 mg/g and 58.479 mg/g, respectively. The Freundlich isotherm's R^2 value for each adsorbent was lower than Langmuir isotherm indicating that it was not applicable to the adsorption of diclofenac. In addition, the value of n for each adsorbent is less than 1. If the value of n is between 2 and 10, the adsorption is good; if it is between 1 and 2, the adsorption is roughly challenging; and if it is less than 1, the adsorption is poor (Oumabady et al. 2022).

ADSORPTION KINETICS

In this study, adsorption kinetics was described using two kinetics models which were pseudo-first-order and pseudo-second-order. The pseudo-first-order equation represented by Equation (6) in its linearized form:

$$\log q_e - q_t = \log q_e - \frac{K_1}{2.303}t \quad (6)$$

TABLE 3. Isotherm parameters of diclofenac adsorption

Isotherms models	Parameters	Samples		
		Poly(ACN-*co*-AAc)	ETA-functionalized poly(ACN-*co*-AAc)	EDA-functionalized poly(ACN-*co*-AAc)
Langmuir Isotherms	q_m (mg g^{-1})	58.479	120.482	80.645
	K_L (mg/mg)	0.0208	0.0245	0.0383
	R^2	0.9938	0.9925	0.9939
Freundlich Isotherms	K_F (L mg^{-1})	0.8296	1.0164	1.3573
	N	0.5164	0.6192	0.5312
	R^2	0.9462	0.9451	0.9658

where K_1 (min^{-1}) is the pseudo-first-order rate constant; and q_e and q_t (mg g^{-1}) are the adsorption capacities at equilibrium and at time t (min), respectively.

The kinetic equation of the pseudo-second-order model can be written in its linearized form as:

$$\frac{t}{q_t} = \frac{1}{k_2 {q_e}^2} + \left(\frac{1}{q_e}\right)t \quad (7)$$

where k is the adsorption rate constant (g mg^{-1} min^{-1}); q_e is the quantity of solute adsorbed at equilibrium (mg g^{-1}); and q_t is the quantity of solute on the surface of the adsorbent at any time t (mg g^{-1}).

As summarized in Table 4, a higher value of R^2 was obtained for second-order kinetic models which were 0.9950 for poly(ACN-*co*-AAc), 0.9930 for ETA-functionalized poly(ACN-*co*-AAc), and 0.9906 for EDA-functionalized poly(ACN-*co*-AAc), respectively. The pseudo-second-order kinetic model best describes that the rate-limiting step of DCF removal is chemisorption (Ensano et al. 2019). The results obtained from the experiment showed that the highest adsorption capacity was ETA-functionalized poly(ACN-*co*-AAc) which was 188.6792 mg/g. Diclofenac adsorption is influenced by electrostatic interactions between diclofenac and positively charged surfaces of adsorbents. Other interactions such as hydrophobic effects and van der Waals forces also contribute to the adsorption of diclofenac onto adsorbents (Oumabady et al. 2022). The calculated values of q_e(calc) were compared with the experimental data, q_e(exp). It was showed that the predicted value of adsorption capacity (q_e (calc)) by pseudo-first-order showed a great difference from the q_e(exp) compared to the pseudo-second-order. Based on the results of the pseudo-second-order model as the governing kinetics model, it represents the slow step in the process of interaction (the formation of the bond) between adsorbate and adsorbent active sites. However, the pseudo-second-order model does not provide the ability to differentiate between physical adsorption, including electrostatic interactions, and chemical adsorption (Cuccarese et al. 2021).

TABLE 4. Kinetic parameters of diclofenac adsorption

Kinetic models	Parameters	Samples		
		Poly(ACN-*co*-AAc)	ETA-functionalized poly(ACN-*co*-AAc)	EDA-functionalized poly(ACN-*co*-AAc)
Pseudo-first-order	k_1 (min^{-1})	0.000390	0.002055	0.000282
	q_e(calc) (mg g^{-1})	1.05535	1.32831	1.03966
	q_e(exp) (mg g^{-1})	140.7156	180.3312	173.025
	R^2	0.8508	0.8175	0.8446
Pseudo-second-order	k_2 (g min^{-1} min^{-1})	1.25374×10^6	2.57970×10^6	1.83654×10^6
	q_e(calc) (mg g^{-1})	147.0588	188.6792	181.8182
	q_e(exp) (mg g^{-1})	140.7156	180.3312	173.025
	R^2	0.9950	0.9930	0.9906

PROPOSED MECHANISMS OF DICLOFENAC ADSORPTION BY AMINE-FUNCTIONALIZED POLY(ACN-co-AAc)

Figure 9 represents the proposed mechanism of adsorption of amine-functionalized poly(ACN-*co*-AAc) adsorbents. The adsorption is mainly contributed by electrostatic interaction between the surface of adsorbents and DCF molecules. The attraction of the lone pair of nitrogen atom obtained from the nitrile group of functionalized polymer to the hydrogen atom of diclofenac molecules results in the formation of electrostatic attraction. In addition, attraction of lone pair of oxygen atoms of diclofenac molecules to the hydrogen atom of amine-functionalized poly(ACN-*co*-AAc) molecules also formed by electrostatic attraction (Shaipulizan et al. 2020).

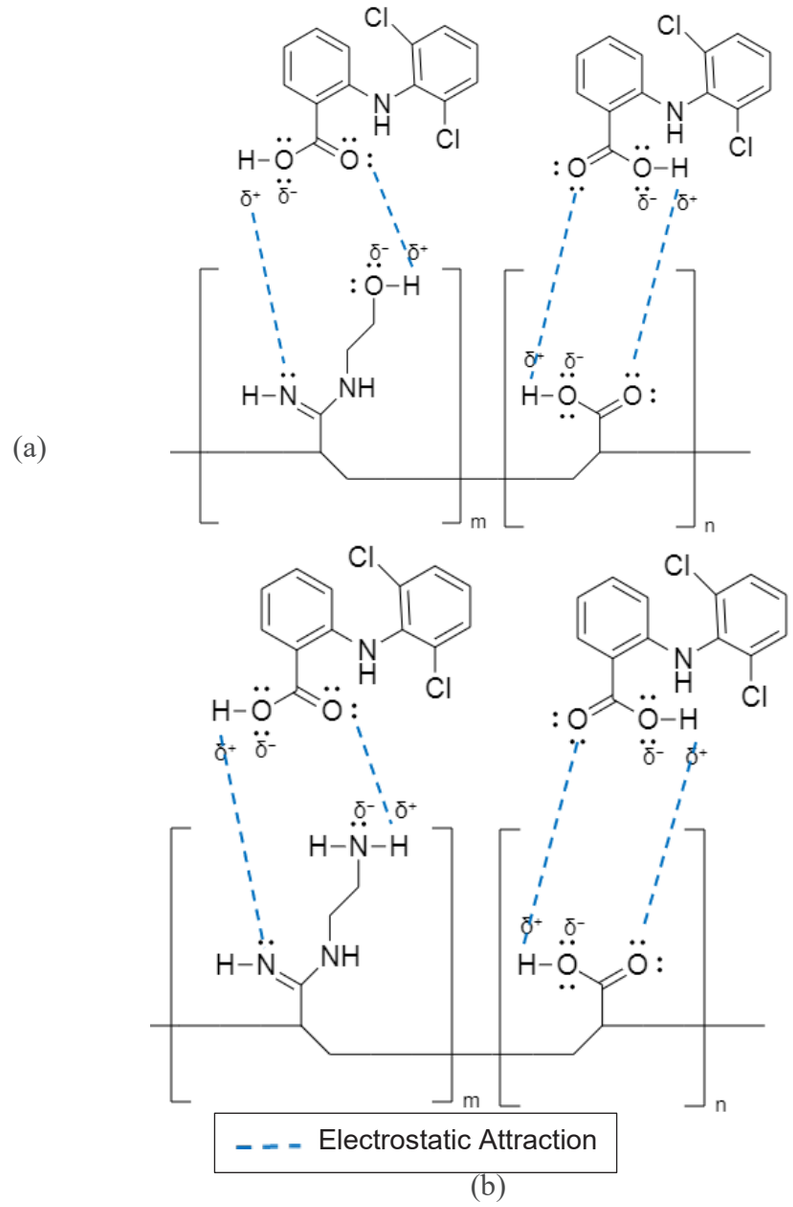

FIGURE 9. Proposed interaction mechanism of diclofenac (DCF) toward the active sites of (a) ETA-functionalized poly(ACN-*co*-AAc) and (b) EDA-functionalized poly(ACN-*co*-AAc)

Conclusions

PAN and poly(ACN-*co*-AAc) were successfully synthesized through redox polymerization, with the presence of sodium bisulphate (SBS) and potassium persulphate (KPS) as initiators. The yield of polymerization for PAN was 96% while for poly(ACN-*co*-AAc) was 94%. The poly(ACN-*co*-AAc) was successfully chemically functionalized using ethanolamine and ethylenediamine as modification agents. The FTIR results showed that the nitrile group (C≡N) in both amine-functionalized poly(ACN-*co*-AAc) disappeared, and the new absorption bands formed in the range 1643-1629 cm^{-1} that were indicated to the C=N stretching that overlapped with the C=O stretching, confirming the success of the surface modification. SEM micrographs showed that the amine-functionalized poly(ACN-*co*-AAc) remained in spherical microspheres after modification occurred. The TGA results show that both poly(ACN-*co*-AAc) functionalized with amine group decomposed at a lower temperature compared to unfunctionalized copolymer. The functionalization of poly(ACN-*co*-AAc) leads to a reduction of surface area and pore volume and increments the pore size.

The effect of pH, adsorbent dosage, initial concentration, and contact time were carried out. The results showed that the optimum pH for both amine-functionalized poly(ACN-*co*-AAc) were pH 7. Moreover, the percentage removal and adsorption capacities increase as the initial concentration increases. The same trend was observed with the adsorbent dosage. The copolymer functionalized with EDA reaches equilibrium at 25th min with 90% of percentage removal and 180.2 mg/g for adsorption capacity. Meanwhile, in the case of ETA- functionalized poly(ACN-*co*-AAc), the equilibrium was achieved at 30th min with 86% of percentage removal and 173.3 mg/g for adsorption capacity. The data showed that the Langmuir isotherm model is the best to describe the isotherm behaviour for the adsorption of diclofenac on the surface of both adsorbents showing that the monolayer adsorption process was preferable. The kinetic studies showed that the adsorption process followed the pseudo-second-order model and underwent the chemisorption process.

Acknowledgements

Thanks are due to the Chemistry Department, Faculty of Science, Universiti Putra Malaysia (UPM) for providing research facilities. The research work is funded by Ministry of Higher Education (MOHE) Malaysia with grand code FRGS/1/2016/TK05/UPM/02/1 (MOHE reference) and UPM reference of UPM/700-2/1/FRGS/03-01-16-1844FR.

References

Adelli, G.R., Balguri, S.P., Bhagav, P., Raman, V. & Majumdar, S. 2017. Diclofenac sodium ion exchange resin complex loaded melt cast films for sustained release ocular delivery. *Drug Delivery* 24(1): 370-379. https://doi.org/10.1080/10717544.2016.1256000

Adeyi, A.A., Jamil, S.N.A.M., Abdullah, L.C., Choong, T.S.Y., Lau, K.L. & Abdullah, M. 2019. Simultaneous adsorption of cationic dyes from binary solutions by thiourea-modified poly(acrylonitrile-co-acrylic acid): Detailed isotherm and kinetic studies. *Materials* 12(18): 2903. https://doi.org/10.3390/ma12182903

AL-Kindi, G.Y., AL Ani, F.H., Al-Bidri, N.K. & Alhaidri, H.A. 2021. Diclofenac removal from wastewater by activated carbon. *IOP Conference Series: Earth and Environmental Science* 779(1): 012091. https://doi.org/10.1088/1755-1315/779/1/012091

Alessandretti, I., Rigueto, C.V.T., Nazari, M.T., Rosseto, M. & Dettmer, A. 2021. Removal of diclofenac from wastewater: A comprehensive review of detection, characteristics and tertiary treatment techniques. *Journal of Environmental Chemical Engineering* 9(6): 106743. https://doi.org/10.1016/j.jece.2021.106743

Angosto, J.M., Roca, M.J. & Fernández-López, J.A. 2020. Removal of diclofenac in wastewater using biosorption and advanced oxidation techniques: Comparative results. *Water* 12(12): 3567. https://doi.org/10.3390/w12123567

Aoopngan, C., Nonkumwong, J., Phumying, S., Promjantuek, W., Maensiri, S., Noisa, P., Pinitsoontorn, S., Ananta, S. & Srisombat, L. 2019. Amine-functionalized and hydroxyl-functionalized magnesium ferrite nanoparticles for congo red adsorption. *ACS Applied Nano Materials* 2(8): 5329-5341. https://doi.org/10.1021/acsanm.9b01305

Ayawei, N., Ebelegi, A.N. & Wankasi, D. 2017. Modelling and interpretation of adsorption isotherms. *Journal of Chemistry* 2017: 3039817. https://doi.org/10.1155/2017/3039817

Bonnefille, B., Gomez, E., Courant, F., Escande, A. & Fenet, H. 2018. Diclofenac in the marine environment: A review of its occurrence and effects. *Marine Pollution Bulletin* 131: 496-506. https://doi.org/10.1016/j.marpolbul.2018.04.053

Christian, N., Manga, N., Raoul, T. & Gabche, A. 2017. Optimisation of activated carbon preparation by chemical activation of ayous sawdust, cucurbitaceae peelings and hen egg shells using response surface methodology. *International Research Journal of Pure and Applied Chemistry* 14(4): 1-12. https://doi.org/10.9734/irjpac/2017/36021

Chu, Y., Khan, M.A., Xia, M., Lei, W., Wang, F. & Zhu, S. 2019. Synthesis and mechanism of adsorption capacity of modified montmorillonite with amino acids for 4-acetaminophenol removal from wastewaters. *Journal of Chemical & Engineering Data* 64(12): 5900-5909. https://doi.org/10.1021/acs.jced.9b00795

Cuccarese, M., Brutti, S., De Bonis, A., Teghil, R., Mancini, I.M., Masi, S. & Caniani, D. 2021. Removal of diclofenac from aqueous solutions by adsorption on thermo-plasma expanded graphite. *Scientific Reports* 11(1): 3427. https://doi.org/10.1038/s41598-021-83117-z

Ensano, B.M.B., de Luna, M.D.G., Rivera, K.K.P., Pingul-Ong, S.M.B. & Ong, D.C. 2019. Optimization, isotherm, and kinetic studies of diclofenac removal from aqueous solutions by Fe–Mn binary oxide adsorbents. *Environmental Science and Pollution Research* 26(31): 32407-32419. https://doi.org/10.1007/s11356-019-06514-y

Ghavi, F.P., Raouf, F. & Koohi, A.D. 2020. The effect of alkaline pretreatment on surfactant-modified clinoptilolite for diclofenac adsorption: Isotherm, kinetic, and thermodynamic studies. *Journal of Water and Health* 19(1): 47-66. https://doi.org/10.2166/wh.2020.057

Göktaş, M. 2020. Copolymer synthesis with redox polymerization and free radical polymerization systems. In *Redox*, edited by Khattak, R. Intechopen https://doi.org/10.5772/intechopen.88088

Gorzin, F. & Abadi, M.B.R. 2017. Adsorption of Cr(VI) from aqueous solution by adsorbent prepared from paper mill sludge: Kinetics and thermodynamics studies. *Adsorption Science & Technology* 36(1-2): 149-169. https://doi.org/10.1177/0263617416686976

Guo, Y., Qi, P.S. & Liu, Y.Z. 2017. A review on advanced treatment of pharmaceutical wastewater. *IOP Conference Series: Earth and Environmental Science* 63: 012025. https://doi.org/10.1088/1755-1315/63/1/012025

Jamil, S.N.A.M., Daik, R. & Ahmad, I. 2010. Preparation and thermal behaviour of acrylonitrile (AN)/ethyl acrylate (EA) copolymer and acrylonitrile (AN)/ethyl acrylate (EA)/fumaronitrile (FN) terpolymer as precursors for carbon fibre. *Pertanika J. Sci. & Technol*. 18(2): 401-409. http://www.pertanika.upm.edu.my/resources/files/Pertanika%20PAPERS/JST%20Vol.%2018%20(2)%20Jul.%202010/19%20Pg%20401-409.pdf

Jodeh, S., Abdelwahab, F., Jaradat, N., Warad, I. & Jodeh, W. 2016. Adsorption of diclofenac from aqueous solution using *Cyclamen persicum* tubers based activated carbon (CTAC). *Journal of the Association of Arab Universities for Basic and Applied Sciences* 20(1): 32-38. https://doi.org/10.1016/j.jaubas.2014.11.002

Khan, A. & Anwer, M. 2020. Advance techniques for diclofenac removal from pharmaceutical wastewater: A review. *International Research Journal on Advanced Science Hub* 2(Special Issue ICIES 9S): 26-31. https://doi.org/10.47392/irjash.2020.154

Kołodziejska, J. & Kołodziejczyk, M. 2018. Diclofenac in the treatment of pain in patients with rheumatic diseases. *Reumatologia* 56(3): 174-183. https://doi.org/10.5114/reum.2018.76816

Kurniawati, D., Bahrizal, Sari, T.K., Adella, F. & Sy, S. 2021. Effect of contact time adsorption of rhodamine B, methyl orange and methylene blue colours on langsat shell with batch methods. *Journal of Physics: Conference Series* 1788(1): 012008. https://doi.org/10.1088/1742-6596/1788/1/012008

Lara-Pérez, C., Leyva, E., Zermeño, B., Osorio, I., Montalvo, C. & Moctezuma, E. 2020. Photocatalytic degradation of diclofenac sodium salt: Adsorption and reaction kinetic studies. *Environmental Earth Sciences* 79: 277. https://doi.org/10.1007/s12665-020-09017-z

Leone, V.O., Pereira, M.C., Aquino, S.F., Oliveira, L.C.A., Correa, S., Ramalho, T.C., Gurgel, L.V.A. & Silva, A.C. 2017. Adsorption of diclofenac on a magnetic adsorbent based on maghemite: Experimental and theoretical studies. *New Journal of Chemistry* 42(1): 437-449. https://doi.org/10.1039/C7NJ03214E

Liang, X.X., Omer, A.M., Hu, Z., Wang, Y., Yu, D. & Ouyang, X. 2019. Efficient adsorption of diclofenac sodium from aqueous solutions using magnetic amine-functionalized chitosan. *Chemosphere* 217: 270-278. https://doi.org/10.1016/j.chemosphere.2018.11.023

Lonappan, L., Brar, S.K., Das, R.K., Verma, M. & Surampalli, R.Y. 2016. Diclofenac and its transformation products: Environmental occurrence and toxicity - A review. *Environment International* 96: 127-138. https://doi.org/10.1016/j.envint.2016.09.014

Mohammed, S.A., Kahissay, M.H. & Hailu, A.D. 2021. Pharmaceuticals wastage and pharmaceuticals waste management in public health facilities of Dessie town, North East Ethiopia. *PLoS ONE* 16(10): e0259160. https://doi.org/10.1371/journal.pone.0259160

Oumabady, S., Selvaraj, P.S., Periasamy, K., Veeraswamy, D., Ramesh, P.T., Palanisami, T. & Ramasamy, S.P. 2022. Kinetic and isotherm insights of Diclofenac removal by sludge derived hydrochar. *Scientific Reports* 12: 2184. https://doi.org/10.1038/s41598-022-05943-z

Park, O-K., Lee, S., Joh, H-I., Kim, J.K., Kang, P-H., Lee, J.H. & Ku, B-C. 2012. Effect of functional groups of carbon nanotubes on the cyclization mechanism of polyacrylonitrile (PAN). *Polymer* 53(11): 2168-2174. https://doi.org/10.1016/j.polymer.2012.03.031

Popa, A., Borcanescu, S., Holclajtner-Antunović, I., Bajuk-Bogdanović, D. & Uskoković-Marković, S. 2020. Preparation and characterisation of amino-functionalized pore-expanded mesoporous silica for carbon dioxide capture. *Journal of Porous Materials* 28(1): 143-156. https://doi.org/10.1007/s10934-020-00974-1

Qiu, Z., Sun, J., Han, D., Wei, F., Mei, Q., Wei, B., Wang, X., An, Z., Bo, X., Li, M., Xie, J. & He, M. 2020. Ozonation of diclofenac in the aqueous solution: Mechanism, kinetics and ecotoxicity assessment. *Environmental Research* 188: 109713. https://doi.org/10.1016/j.envres.2020.109713

Rapeia, N., Siti, N., Jamil, S.N.A.M., Abdullah, L., Mobarekeh, M., Yaw, T., Huey, S., Zahri, N.A.M. 2015. Preparation and characterization of hydrazine- modified poly(acrylonitrile-co-acrylic acid). *Journal of Engineering Science and Technology Special Issue on SOMCHE 2014 & RSCE 2014 Conference*, January(2015): 61-70. https://jestec.taylors.edu.my/Special%20Issue%204_SOMCHE_2014/SOMCHE%202014_4_2015_061_070.pdf

Sathishkumar, P., Arulkumar, M., Ashokkumar, V., Mohd Yusoff, A.R., Murugesan, K., Palvannan, T., Salam, Z., Ani, F.N. & Hadibarata, T. 2015. Modified phyto-waste *Terminalia catappa* fruit shells: A reusable adsorbent for the removal of micropollutant diclofenac. *RSC Advances* 5(39): 30950-30962. https://doi.org/10.1039/c4ra11786g

Shaipulizan, N.S., Md Jamil, S.N.A., Kamaruzaman, S., Subri, N.N.S., Adeyi, A.A., Abdullah, A.H. & Abdullah, L.C. 2020. Preparation of ethylene glycol dimethacrylate (EGDMA)-Based terpolymer as potential sorbents for pharmaceuticals adsorption. *Polymers* 12(2): 423. https://doi.org/10.3390/polym12020423

Venkatakrishnan, A. & Kuppa, V.K. 2018. Polymer adsorption on rough surfaces. *Current Opinion in Chemical Engineering* 19: 170-177. https://doi.org/10.1016/j.coche.2018.03.001

Yaghmaeian, K., Yousefi, N., Bagheri, A., Mahvi, A.H., Nabizadeh, R., Dehghani, M.H., Fekri, R. & Akbari-Adergani, B. 2022. Combination of advanced nano-Fenton process and sonication for destruction of diclofenac and variables optimization using response surface method. *Scientific Reports* 12(1): 20954. https://doi.org/10.1038/s41598-022-25349-1

Yusuff, A.S. 2019. Adsorption of hexavalent chromium from aqueous solution by *Leucaena leucocephala* seed pod activated carbon: Equilibrium, kinetic and thermodynamic studies. *Arab Journal of Basic and Applied Sciences* 26(1): 89-102. https://doi.org/10.1080/25765299.2019.1567656

Zahri, N.M., Md Jamil, S., Abdullah, L., Shean Yaw, T., Nourouzi Mobarekeh, M., Sim, J. & Mohd Rapeia, N. 2015. Improved method for preparation of amidoxime modified poly(acrylonitrile-co-acrylic acid): Characterizations and adsorption case study. *Polymers* 7(7): 1205-1220. https://doi.org/10.3390/polym7071205

Zhu, Y., Liang, H., Yu, R., Hu, G. & Chen, F. 2020. Removal of aquatic cadmium ions using thiourea modified poplar biochar. *Water* 12(4): 1117. https://doi.org/10.3390/w12041117

*Corresponding author; email: ctnurulain@upm.edu.my